PCCP

On the mechanism for the reduction of nitrogen monoxide on Rh(111) single-crystal surfaces

Francisco Zaera* and Chinnakonda S. Gopinath†

Department of Chemistry, University of California, Riverside, Riverside, California 92521, USA

Received 19th August 2002, Accepted 10th December 2002
First published as an Advance Article on the web 3rd January 2003

Isothermal kinetic experiments were carried out with isotopically-labeled molecular beams in order to characterize the surface reactions involved in the reduction of nitrogen monoxide with carbon monoxide on Rh(111) single-crystal surfaces. The new data reported here offers support for the basic model advanced previously where N_2 production takes place *via* the formation of N–NO intermediates at the periphery of atomic nitrogen surface islands. However, they also highlight a few additional subtle complications. In particular, the rapid desorption of a small amount of $^{14}N^{14}N$ upon switching from $^{14}NO + CO$ to $^{15}NO + CO$ mixtures points to the role of additional adsorbates nearby the reaction surface site in facilitating the dissociation of the N–NO intermediates. In addition, the results from experiments with mixed $^{14}NO + {}^{15}NO + CO$ indicate a combination of reactions at the edges of previously deposited ^{14}N islands and the growth of new mixed $^{14}N + {}^{15}N$ surface clusters.

1. Introduction

The fundamental chemistry of nitrogen oxides, of NO in particular, on rhodium surfaces is of great importance for the catalysis of air pollution control, and has been extensively studied in the past.[1–3] Early surface-science experiments on Rh(111) under vacuum indicated that the mechanism of the conversion of NO to N_2 on the surface is fairly complex.[4–21] Temperature programmed desorption data have shown that the desorption of molecular nitrogen from NO decomposition on Rh(111) occurs in two stages, around 470 and above 500 K.[4,22–26] Particularly puzzling is the fact that the first TPD N_2 peak at 470 K does not shift in temperature with changing coverages, a behavior generally associated with first-order processes. Nevertheless, experiments with different surface-sensitive techniques[23–26] have shown that NO dissociation occurs at quite low temperatures, below 300 K at low coverages and around 450 K at high coverages. This strongly suggests that the rate of catalytic reduction of NO is determined by the mechanism of N_2 formation on the surface.

Additional clues on the microscopic details of NO conversion processes have come from studies carried out at moderate pressures.[10,11,17,27] Most commercial Rh/Al_2O_3 automotive catalysts are quite selective towards N_2 production,[15,18,20] but some N_2O formation has been detected in atmospheric-pressure single-crystal studies.[11] Fisher and co-workers,[4,5,7–9,25] in their initial studies in the mid-eighties, proposed two separate pathways for this, the generally accepted recombination of nitrogen atoms on the surface, and a disproportionation between adsorbed NO and N which could also account for the formation of the N_2O. Newer experimental data by Belton *et al.*[10,11,17,27,28] argued that the latter reaction does in fact not occur on Rh(111), at least under vacuum. Finally, a few kinetic experiments with molecular beams have been reported on Rh(111)[29] and Rh(110)[30] as well as on palladium particles supported on MgO.[31]

We over the past few years have carried out a number of molecular beam experiments on Rh(111) single-crystal surfaces to address these and other issues related to the mechanism of the reduction of NO to molecular nitrogen.[22,32–41] Particularly insightful have been the data obtained from isothermal kinetic investigations carried out using isotope labeling. Both the characterization of the transient kinetic behavior during $NO + CO$ conversion on Rh(111) and temperature-programmed desorption (TPD) post-mortem analysis of the remaining surface species were used to identify two types of kinetically different nitrogen atoms during the steady-state conversion of NO to N_2.[32–34] Isotope switching experiments indicated that those two species do not represent nitrogen atoms in different adsorption sites, but rather similar states with adsorption energetics modified by their immediate surroundings on the surface.[33,35,38] Those results can be nicely explained by preferential reactivity at the periphery of nitrogen surface islands, and by molecular nitrogen production *via* the formation of an N–NO intermediate.

Here we expand on our previous isotope switching molecular beams experiments on the $NO + CO$ reaction over Rh(111) surfaces. Additional results are provided below to supplement the evidence previously provided for our island-formation model, but also to highlight further complications in the kinetics of molecular nitrogen formation. Indeed, the rate of N_2 formation in the transient once the surface is no longer exposed to the reactants displays at least two kinetic components. Furthermore, a finite amount of residual ^{14}N–^{14}NO intermediates appears to remain on the surface, and to decompose and produce $^{14}N^{14}N$ only when the surface is re-exposed to the reactant mixture. Experiments with isotopically mixed $^{14}NO + {}^{15}NO + CO$ beams were used to identify other subtle effects associated with the energetic changes induced by neighboring adsorbates.[42–44]

2. Experimental

The apparatus used in the experiments reported here has been described in detail elsewhere.[45,46] Briefly, the stainless-steel ultrahigh vacuum (UHV) vessel is pumped to a base pressure below 2×10^{-10} Torr, and is equipped with a computer-controlled mass quadrupole for gas identification, kinetic

† Present address: National Chemical Laboratory, Pune, India

 DOI: 10.1039/b208091e

determinations, and temperature-programmed desorption (TPD) experiments. A collimated multi-channel micro-capillary array doser 1.2 cm in diameter is used for directional exposure of the sample to the reactants, a sputtering ion gun for sample cleaning, and a crystal holder for three-dimensional translation and on-axis rotation as well as for resistive heating and liquid nitrogen cooling. The Rh(111) single-crystal, a 1.10×0.56 cm^2 rectangle, is cleaned *in-situ*, initially by Ar^+ sputtering and before each experiment by cycles of oxygen exposures (1×10^{-7} Torr at 900 K for up to 20 min) and annealing to 1200 K until the NO TPD spectra reported in the literature[22] can be reproduced. The surface temperature is set by resistive heating using a home-made precision temperature controller, and monitored continuously with a chromel–alumel thermocouple spot-welded to the back of the crystal. Isothermal kinetic experiments were carried out by using a variation of the so-called King and Wells molecular beam method, as described before.[46–48] Unless otherwise specified, all kinetic runs discussed below were performed at a crystal temperature of 480 K, and all TPD were obtained by using a linear heating ramp of 10 K s^{-1}. Isotopically labeled ^{15}NO (CIL, 98% ^{15}N purity) and ^{13}CO (CIL, 99% ^{13}C purity) and regular ^{14}NO (Matheson, 99.9% purity) and ^{12}CO (Matheson, 99.9% purity) were used as supplied.

3. Results

3.1. General experimental considerations

Fig. 1 displays typical raw data from the type of experiments described in this report. Shown is the time evolution of the partial pressures of $^{14}N^{14}N$ and $^{13}CO_2$ during the different stages of an isothermal kinetic run with NO + ^{13}CO mixtures (two similar sets of experiments are needed to obtain data such as these, with ^{12}CO and ^{13}CO, in order to get around the problem of mass interference between $^{14}N^{14}N$ and ^{12}CO and between $^{14}N^{15}N$ and ^{13}CO). The sequence of events in these runs was as follows. First, a 1 : 1 ^{14}NO : ^{13}CO beam was turned on at $t = 5$ s while the flag was kept in the blocking position. Under those conditions, scattering of the beam from the flag leads to increases in the partial pressures of the gases to new steady-state values. Then, the flag was removed at $t = 10$ s in order to allow the beam to impinge directly on the surface. A transient behavior is observed over the following ~10 s, in particular a sharp rise in the $^{13}CO_2$ pressure followed by its return to the final steady-state value. The steady state reached afterwards was checked by blocking the beam with the flag between $t = 60$ and 80 s. It has previously been determined that, at this point, a steady-state coverage of strongly-bonded atomic nitrogen of $\Theta_N \sim 0.17$ monolayers (ML) is present on the surface, and that no significant amount of adsorbed oxygen remains.[33,34]

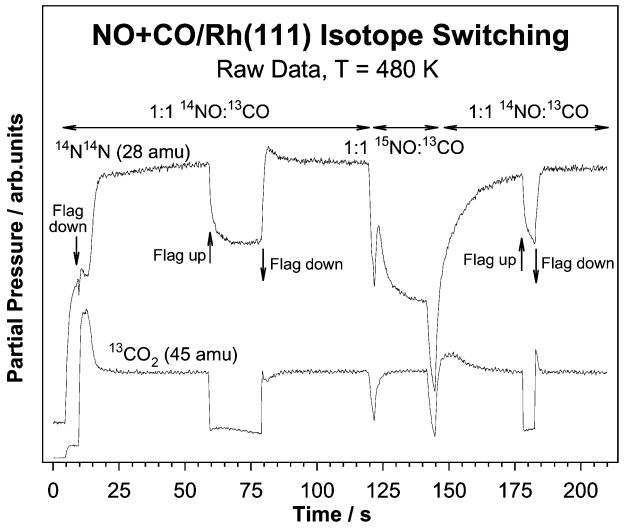

Fig. 1 Raw data ($^{14}N^{14}N$ and $^{13}CO_2$ production rate *versus* time) from a typical isotope-switching isothermal kinetic molecular-beam experiment of the type used in the studies reported here. In this example, the Rh(111) surface was kept at a constant temperature of 480 K, and exposed sequentially to 1 : 1 ^{14}NO : ^{13}CO, ^{15}NO : ^{13}CO, and back to ^{14}NO : ^{13}CO mixtures. A few observations are worth highlighting from the data. First, the same steady-state rates are seen all throughout the kinetic run, as indicated by the similar dips in CO_2 signal observed when the beam is interrupted. Second, the transient kinetics once the reaction beam is blocked is quite fast as far as the production of carbon dioxide is concerned, but much slower for the case of molecular nitrogen desorption. Lastly, a fast exchange of ^{14}NO + CO by ^{15}NO + CO leads to the immediate desorption of a small amount of residual $^{14}N^{14}N$ from the surface.

At $t = 120$ s, the original ^{14}NO + ^{13}CO beam was turned off by pumping on the backing gas manifold (by switching the 5-way valve used to select the gas mixture to the pumping position), and at $t = 121$ s the new ^{15}NO + ^{13}CO beam was introduced (by switching the 5-way valve to the next position). The 1 s interval between the old an new beams is the minimum time needed to ensure that the beam source is completely pumped before injecting the new gases, thus avoiding any isotopic contamination. The reaction was then run for an additional variable period of time Δt, 21 s in this example. In most experiments, the beam was shut off completely after the Δt run with the second beam, and the system was then pumped to its base pressure and nitrogen TPD spectra were taken. However, in the experiment in Fig. 1, another switchover, back to the original beam, was carried out between $t = 142$ and 144 s, and a final check of the steady state conditions (flag up and flag down) was performed between $t = 178$ and 183 s before the post-mortem TPD analysis. In any case, of particular relevance to the discussion offered below is the fact that, since exposures of the surface to the second reaction beam were carried out under the same steady-state reaction conditions used for the initial deposition of the ^{14}N atoms, the total surface coverages remain the same all throughout these experiments; the only changes that take place are in the isotopic composition of the nitrogen overlayers.

3.2. Initial results

Experiments such as that described above in connection with Fig. 1 are rich in kinetic data. For one, the rate of molecular nitrogen production can be measured directly from the transient behavior after interrupting the beam during the steady-state conditions, at $t = 60$ s. Fig. 2 displays the resulting plot of rate *versus* time obtained by averaging eight independent kinetic runs. The data are shown in semilogarithmic fashion to better aid in the estimation of a rate law, and 95% confidence error bars are provided to indicate the reliability of the analysis. It can be seen that the experimental results follow first-order kinetics with respect to the surface atomic nitrogen that desorbs, albeit only after the first ~2 s of reaction following the blocking of the beam. The best first-order fit (solid line) corresponds to a half-life time of *ca.* 2.2 ± 0.2 s. However, it is clear that a second, faster process takes place in the initial 2-s period, and that the first-order rate law can only account for about half of the steady-state nitrogen production rate. Second-order kinetics (dashed line) does not describe this process well at all.

Fig. 3 displays a summary of the data obtained from isotope switching experiments in the form of the temporal evolution of the removal of ^{14}N atoms from the surface during the steady-state conversion of nitrogen monoxide once the original ^{14}NO + CO reacting mixture is replaced by a similar ^{15}NO + CO beam.[33,35,38] Results from two types of experiments are

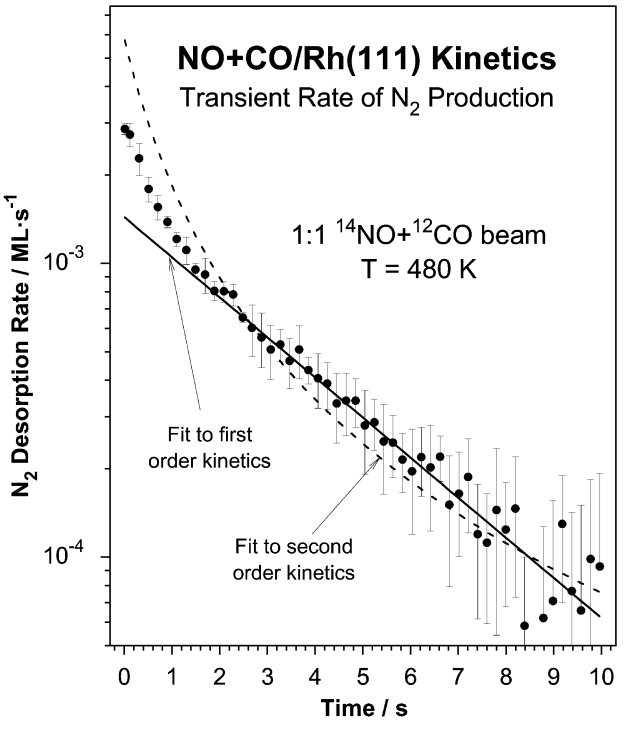

Fig. 2 Transient kinetics for the production of molecular nitrogen following the interruption of the exposure of the Rh(111) surface to the NO + CO reactive beam, extracted from raw traces such as that seen between $t = 60$ and 70 s in Fig. 1, and averaged over several (8) runs for better signal-to-noise (the error bars correspond to a 95% confidence limit). Two kinetic regimes can be easily identified, a first-order rate law associated with the time evolution of the N_2 desorption rate after the first couple of seconds from beam interruption (solid line), and an additional signal at the beginning of the data which accounts for at least half of the nitrogen steady-state production rate. Second order kinetics deviates significantly from the data (dashed line).

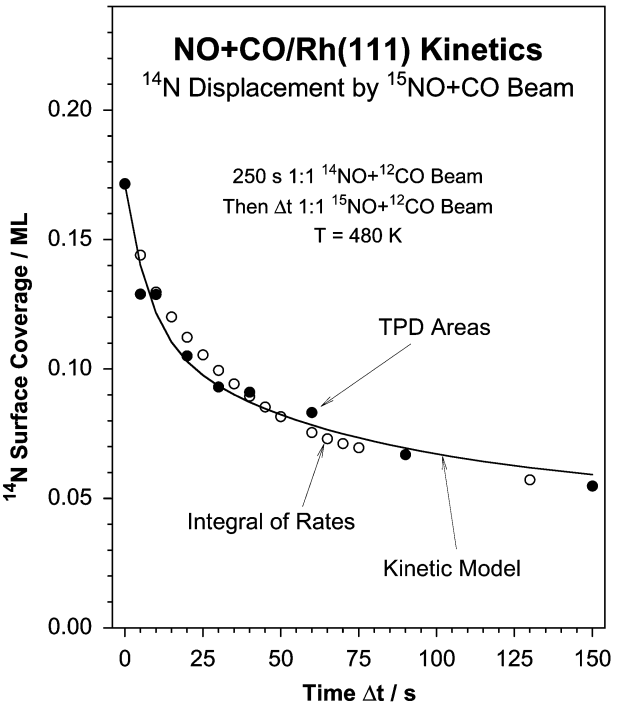

Fig. 3 Temporal behavior of the coverage of atomic nitrogen adsorbed on a Rh(111) single-crystal surface during isotope switching isothermal kinetic experiments. Shown is the evolution of the coverage of ^{14}N adsorbed during the steady-state conversion of a $^{14}NO + CO$ reaction mixture as a function of the time elapsed after switching to a similar $^{15}NO + CO$ beam, all at 480 K. The two sets of data correspond to direct measurements by post-mortem temperature-programmed desorption (TPD) experiments (filled circles), and to integration of the steady-state reaction rates determined by blocking the reaction beam (open circles). Reasonable agreement is seen between the two within the margins of error of the experiments. The complex kinetic is explained by a surface islanding model developed in previous publications,[33,35] as illustrated by the solid curve.

displayed there. First, the isotopic composition of the atomic nitrogen layer present on the surface as a function of the time elapsed after the reaction mixture switchover, obtained *via* post-mortem TPD, are shown as filled circles in Fig. 3. Those data clearly indicate that the ^{14}N replacement by ^{15}N on the rhodium surface during the steady-state conversion of NO + CO mixtures does not follow a simple rate law, and is not complete even after long reaction times with $^{15}NO + CO$ mixtures. Second, the removal of ^{14}N from the surface, calculated by integration of the molecular nitrogen steady-state rates acquired by interrupting the beam flux to the surface and following the resulting kinetic transient directly during the isothermal kinetic runs, is plotted as open circles. The results from the second type of experiments also point to the predominance of ^{14}N removal *via* $^{14}N^{15}N$ formation, implying the involvement of at least one undissociated NO molecule in the mechanism of molecular nitrogen formation.[35] Finally, a fit of the experimental data to our islanding model is displayed as a solid line. Almost no adjustable parameters were used in the calculations associated with this fit, since the island size was independently estimated by the isotope distribution of the molecular nitrogen in the TPD experiments (and was found to not affect the ^{14}N replacement kinetic results significantly anyway), and the desorption rate constant was measured by separate transient kinetic experiments. The only truly adjustable parameter was p, the probability of desorption from the second shell of the island.[33]

3.3. ^{14}N displacement

The ability to rapidly switch between two reaction mixtures in the molecular beam used for the kinetic studies, thanks to the use of a 5-way valve, allows for the detection of fast changes in isotopic composition of the surface species during steady-state catalysis. In our previous reports it was stated that almost all the ^{14}N deposited on the surface is removed as $^{14}N^{15}N$ once the beam labeling is changed from $^{14}NO + CO$ to $^{15}NO + CO$.[33] Nevertheless, the raw data in Fig. 1 indicate that a small amount of $^{14}N^{14}N$ does desorb at the very start of the exposure of the surface to the second beam: notice the spike in the $^{14}N^{14}N$ trace recorded about $t = 125$ s. Integration of that spike in experiments performed as a function of the delay time Δt between the beam switchover and the unblocking of the beam indicate that the amount of $^{14}N^{14}N$ produced in this transient regime decreases with that time. The data are shown as filled circles in Fig. 4. Of interest from these results are the observations that there is always a small amount of residual $^{14}N^{14}N$ produced once the $^{15}NO + CO$ beam is introduced, about 0.007 ML, and that an additional ~0.01 ML can also be detected if the delay time is 1 s or shorter. The time evolution of the coverage of N that desorbs once the first reaction beam is interrupted (the integral of Fig. 2) is also shown in Fig. 4, as a solid line, for comparison. The two sets of data agree quite well as long as the residual 0.007 ML ^{14}N coverage is added to the latter results. This means that not all possible ^{14}N that can desorb as $^{14}N^{14}N$ does so unless the surface is re-exposed to the reaction mixture. This suggests that there may be ^{14}N–^{14}NO adsorbed intermediates left behind, not able to dissociate unless the surrounding surface sites are occupied by other adsorbates. This point will be addressed in more detail in the Discussion section.

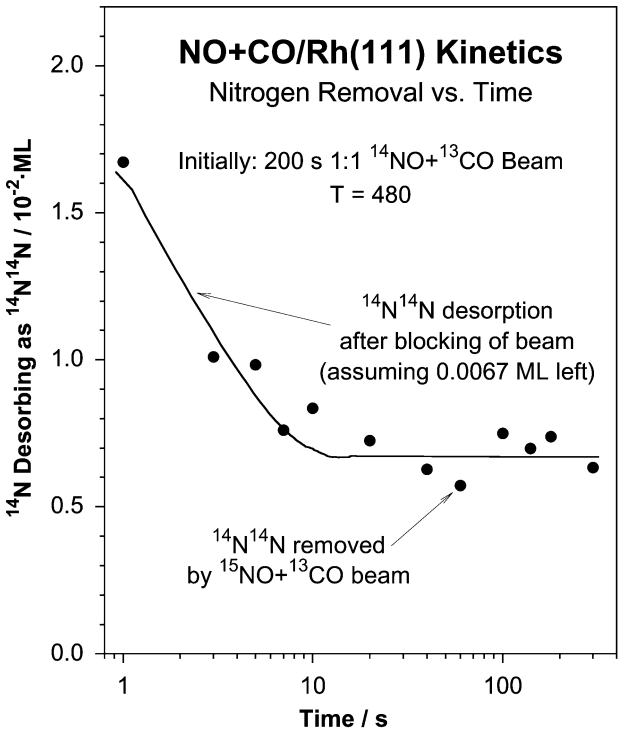

Fig. 4 $^{14}N^{14}N$ desorption yield from two types of experiments: (a) after interruption of the $^{14}NO + {}^{13}CO$ beam once steady-state has been reached, the integral of the data in Fig. 1 (solid line); and (b) after varying delay times following the switch to the $^{15}NO + {}^{13}CO$ beam (filled circles). The first set was offset by 0.0067 ML in order to obtain a reasonable match with the second. This suggests that an amount of residual ^{14}N–^{14}NO intermediates are retained by the surface after the interruption of the reaction with the $^{14}NO + {}^{13}CO$ mixture, and that those can only dissociate and produce $^{14}N^{14}N$ in the presence of new reactants.

The height of the $t = 125$ s spike in Fig. 1 provides an estimate for the maximum rate of desorption of $^{14}N^{14}N$ during these displacement experiments. The value of that rate maximum R_{max} is plotted *versus* delay time, Δt, in the left panel of Fig. 5, and as a function of the total amount of $^{14}N^{14}N$ detected in the right panel of the same figure. R_{max} decreases slowly with Δt, in a semilogarithmic fashion difficult to explain by any simple kinetic model. On the other hand, there is a linear dependence between those rates and the $^{14}N^{14}N$ yields, indicating first-order kinetics: the rate of $^{14}N^{14}N$ production during the transient after isotope switching is proportional to the concentration of the ^{14}N–^{14}NO intermediate left behind on the surface by the first beam. The deviation from linearity seen at the high end of the ^{14}N coverage is due to experimental limitations, since that point corresponds to a delay of $\Delta t = 1$ s, a time comparable to that needed for the switchover.

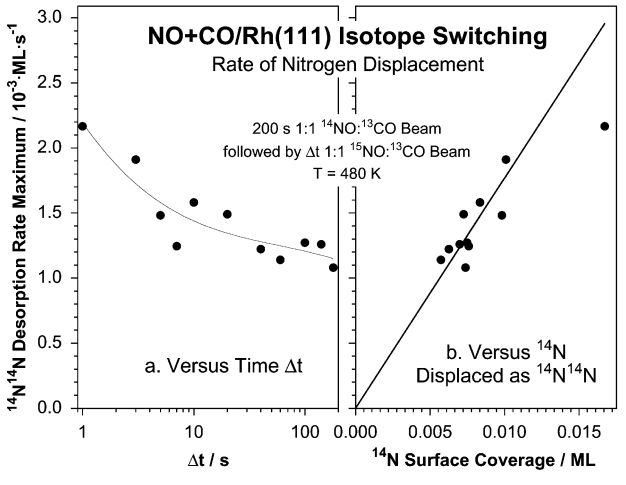

Fig. 5 Rate of $^{14}N^{14}N$ production during the second half of the isotope switching experiments discussed in Figs. 1 and 4, as a function of time delay after the switchover (left), and of the total ^{14}N displaced (right). The temporal changes in $^{14}N^{14}N$ production rate are slow and difficult to describe quantitatively, but depend linearly on the concentration of the surface species leading to the purely ^{14}N-labeled molecular nitrogen.

3.4. Experiments with $^{14}NO + {}^{15}NO$ mixed beams

Additional experiments were carried out with mixed isotope beams. In this case the first beam was still made out of $^{14}NO + CO$ mixtures, but the second contained different combinations of ^{14}NO and ^{15}NO (+CO). The initial idea behind these studies was to corroborate our hypothesis that molecular nitrogen formation requires one new incoming nitrogen monoxide reactant. If that were to be the case, the initial rate for $^{14}N^{14}N$ formation after switching to these isotopically mixed beams should depend linearly on the fraction of ^{14}N in the nitrogen monoxide of the second beam. Unfortunately, since the experiments require to wait for a minimum period of time Δt_{min} after beam switching for reliable rate measurements (because of the variations in background signal during the transient), the results from these studies are more difficult to interpret. Fig. 6 displays the dependence of the rate of $^{14}N^{14}N$ production after $\Delta t = 15$ and 40 s as a function of the fraction of ^{14}NO in the second beam. It can be seen there

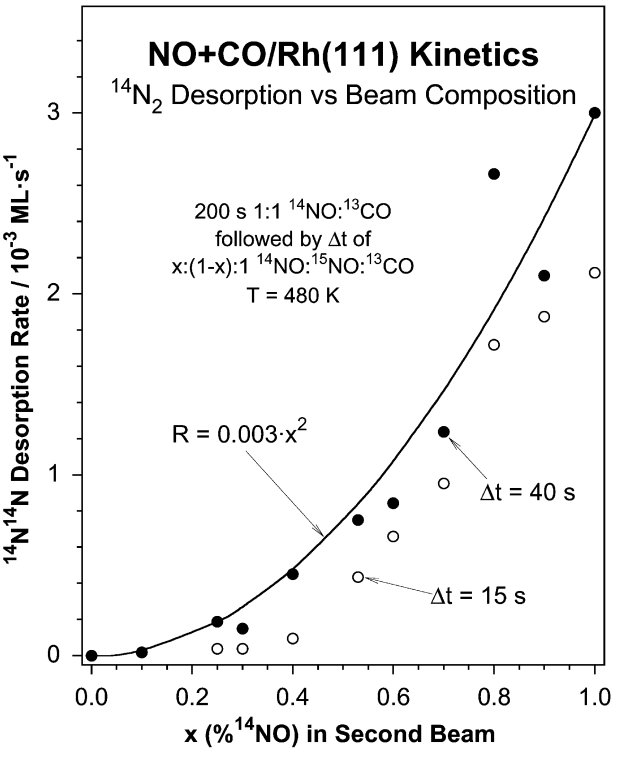

Fig. 6 $^{14}N^{14}N$ production rate dependence on the fraction x of ^{14}NO (from the total nitrogen monoxide) in the $^{14}NO + {}^{15}NO + CO$ mixed beams used in the second part of isothermal kinetic experiments such as that illustrated in Fig. 1. Again, the Rh(111) surface was first exposed to a pure $^{14}NO + {}^{13}CO$ beam until a steady-state condition was reached. Two sets of data are reported for two different delay times after the beam switchover, $\Delta t = 15$ (open circles) and 40 (filled circles) s. The latter follow the second-order behavior expected from steady-state conditions with the second beam (solid line), but the former display a more complex behavior with a threshold x value and a more linear dependence of rate on ^{14}NO fraction.

that the data for $\Delta t = 40$ s can be fitted, within experimental error, to second order kinetics. However, given that after this long period of time of exposure to the second beam, almost half of the surface ^{14}N deposited by the first beam has already been exchanged with ^{15}N and new islands nucleating around new ^{15}N atoms may have started to grow, these data are more reflective of steady-state conditions with the $^{14}NO + {}^{15}NO + {}^{13}CO$.

The data for $\Delta t = 15$ s, the open circles in Fig. 6, are more difficult to understand. There is a clear deviation from second-order behavior in this case, and the results are better described by a linear dependence after an offset at a minimum ^{14}NO fraction of about 0.3. The direct proportionality between $^{14}N^{14}N$ rate production and ^{14}NO fraction in the beam is what is predicted by our islanding model with N–NO intermediate formation at the periphery of the nitrogen islands, but the observation of a minimum ^{14}NO fraction before any $^{14}N^{14}N$ is produced is not as easy to explain. Moreover, it is not clear why the transient ($\Delta t = 15$ s) rates are lower than those seen at later ($\Delta t = 40$ s) times. We have no answers for these questions at the present time.

More information about this system can be extracted from analysis of post-mortem temperature-programmed desorption (TPD) experiments following the use of mixed isotope beams. A typical set of TPD traces obtained after using $^{14}NO + {}^{15}NO + {}^{13}CO$ mixtures in the second beam is presented in Fig. 7, in this case for a 0.3 : 0.7 $^{14}NO : {}^{15}NO$ composition and $\Delta t = 40$ s. The data recorded after a separate experiment where the ^{14}N surface layer was exposed to a $^{15}NO + {}^{13}CO$ beam for $\Delta t = 10$ s are also shown for comparison. Both experiments led to approximately the same level of isotopic exchange within the nitrogen surface layer (~2 : 1 $^{14}N : {}^{15}N$), but to significantly different molecular nitrogen desorption kinetics. In particular, notice the marked shift in temperature maximum in the $^{15}N^{15}N$ trace, from *ca.* 560 K with pure ^{15}NO, to 580 K when the isotopically mixed beam was used instead. According to our islanding model, nitrogen desorption in these TPD experiments occurs layer by layer, starting from the periphery of the atomic nitrogen surface islands and progressing towards the center as the temperature is increased.[38] Consequently, a higher $^{15}N^{15}N$ desorption temperature with the $^{14}NO + {}^{15}NO$ beam is indicative of ^{15}N deposition deeper inside the nitrogen islands. This is consistent with the explanation provided above for the dependence of $^{14}N^{14}N$ formation rate as a function of the extent of isotopic labeling.

A more comprehensive view of the behavior of the temperature maxima in the TPD traces as a function of the fraction of ^{14}N on the surface (with respect to the total adsorbed nitrogen) is presented in Fig. 8 for two sets of experiments: (1) with $^{14}NO + {}^{15}NO + {}^{13}CO$ beams of different compositions, after a fixed $\Delta t = 40$ s; and (2) with pure $^{15}NO + {}^{13}CO$ beams after different Δt's. The display in terms of surface isotope composition allows for a direct comparison between the two sets in terms of equivalent levels of isotope scrambling, even though it should be kept in mind that this requires longer times and implies more extensive total surface nitrogen exchange with the mixed beams. In any case, it is quite apparent that the desorption maxima for the three molecular nitrogen isotopologues display larger differences in the case of the pure ^{15}NO reaction mixture. This implies a higher degree of heterogeneity in the distribution of atomic nitrogen on the surface, specifically the predominance of ^{15}N at the periphery and ^{14}N at the core of the surface islands. More extensive scrambling is seen with the mixed beams because of the longer times of reaction with the second beam.

Finally, Fig. 9 summarizes the results obtained in terms of TPD yields as a function of ^{14}NO fraction in the second beam. The left panel shows the corresponding yields for $^{14}N^{14}N$, $^{14}N^{15}N$, and $^{15}N^{15}N$, while the right frame displays the total fraction of ^{15}N on the surface calculated by using the areas below the TPD traces. All these TPD experiments were carried out after $\Delta t = 40$ s exposures of the surface to the second beam. Interestingly, the extent of the displacement of ^{14}N by ^{15}N does not depend linearly on the amount of ^{15}NO in the beam, but displays a lower kinetic order, somewhere between 0.5 and 1, instead. This is to say that there is a slight bias towards the incorporation of ^{15}N (as opposed to ^{14}N) to the nitrogen surface islands, perhaps because of a kinetic isotope effect (favoring desorption, not dissociation, for ^{14}NO). More to the point of testing our model, the yields for $^{14}N^{15}N$ formation are highly non-linear with respect to the fraction of ^{14}N in the second beam, being almost constant for compositions all the way from pure $^{15}NO + {}^{13}CO$ beams to mixtures where over

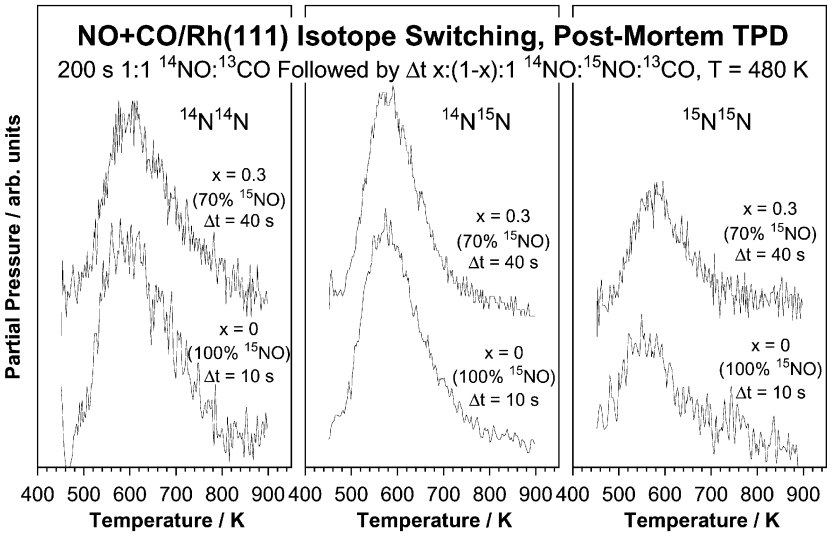

Fig. 7 $^{14}N^{14}N$ (left), $^{14}N^{15}N$ (middle), and $^{15}N^{15}N$ (right) post-mortem temperature-programmed desorption (TPD) spectra from two types of isothermal molecular beam experiments, with 1 : 1 $^{15}NO + {}^{13}CO$ (lower trace) and 0.3 : 0.7 : 1 $^{14}NO + {}^{15}NO + {}^{13}CO$ (upper traces) mixtures in the second beam. The delay times for the second beam before stopping the reaction and acquiring the TPD, $\Delta t = 10$ and 40 s respectively, were chosen to obtain comparable $^{14}N : {}^{15}N$ ratios on the surface (*ca.* 2 : 1). Significant differences are seen between the two sets in terms of TPD peak shapes and temperature maxima. Notice in particular the ~20 K lower peak temperature in the $^{15}N^{15}N$ trace for the pure $^{15}NO + {}^{13}CO$ case, indicative of a more spatially inhomogeneous distribution of atomic nitrogen isotopes on the surface in that case.

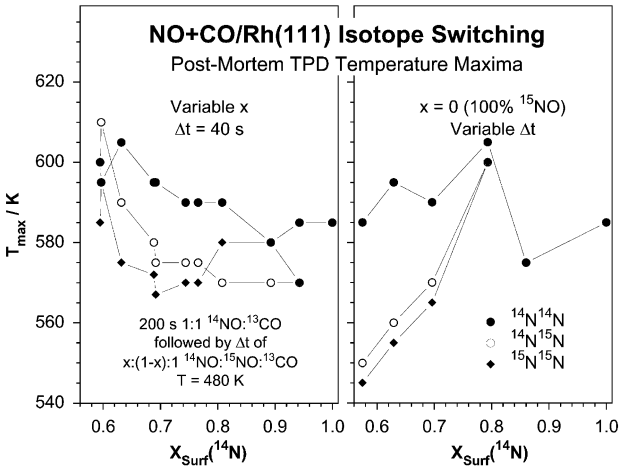

Fig. 8 Post-mortem TPD peak maximum temperatures for $^{14}N^{14}N$, $^{14}N^{15}N$ and $^{15}N^{15}N$ as a function of the ^{14}N fraction of the total atomic nitrogen present on the Rh(111) surface under steady-state conditions. Two sets of data are contrasted here, those obtained by varying the isotopic composition of the second beam while keeping the delay time constant at $\Delta t = 40$ s (left), and *versus* delay time Δt when using pure $^{15}NO + {}^{13}CO$ mixtures. While differences in T_{max} are obvious in the latter case, a more similar behavior is seen for all the isotopologues with the mixed beams, again reflecting differences in the distribution of the nitrogen atoms within the surface between the both cases.

half of the nitrogen monoxide is in the form of ^{14}NO. The line through those data is a fit assuming *ca.* one-third linear dependence (recombination of ^{15}N with ^{14}N at the periphery of the islands produced by the first beam) and two-thirds second-order behavior (recombination from newly deposited $^{14}N + {}^{15}N$ atoms).

3.5. Additional tests

A few additional tests and control experiments were carried out to check the validity of the results presented above. As mentioned before, duplicate experiments were carried out with ^{12}CO and ^{13}CO in order to minimize problems with signal overlap in the mass spectrometer among molecules with the same molecular weight, among $^{14}N^{14}N$ and ^{12}CO and $^{14}N^{15}N$ and ^{13}CO in particular. Agreement between the two sets was always assured by the reproduction of the rate of carbon dioxide formation. Another set of studies was performed using $x:(1-x):1\ ^{14}NO:{}^{15}NO:CO$ beams (two sets with both ^{12}CO and ^{13}CO for each case) in the first part of isothermal kinetic experiments to make sure that there were no experimental artifacts that could taint the observations reported so far. An example of the results from this work is shown in Fig. 10, in that case for a $0.5:0.5:1\ ^{14}NO:{}^{15}NO:CO$ mixture. As expected, the steady-state rates for $^{14}N^{14}N$ and $^{14}N^{15}N$ production follow the ratio estimated based on statistical grounds (0.0008 ML s^{-1} : 0.0016 ML s^{-1}, according to the signal drops after blocking the beam at $t = 140$ s). Also, the post-mortem TPD yields follow the appropriate isotopologue distribution of 0.023 ML : 0.045 ML : 0.022 ML, and all three TPD traces display similar shapes and temperature maxima.

Finally, a few experiments were carried out where two beam switches were performed, from a $^{14}NO:CO$ mixture to a similar $^{15}NO:CO$ beam after 200 s of data collection, and back to the original $^{14}NO:CO$ for another 200 s after a variable Δt_2 period with the intermediate beam. The post-mortem nitrogen TPD traces obtained for the case of $\Delta t_2 = 40$ s are shown in the main frame of Fig. 11. Only a little over 20% of the surface nitrogen is ^{15}N in that case, since the rest is displaced *via* $^{14}N^{15}N$ formation by the third $^{14}NO:CO$ mixture. Nevertheless, the $^{15}N^{15}N$ TPD trace displays two marked and well-separated features around 550 and >700 K. This behavior, not seen in any of the other experiments, indicates two distinct types of ^{15}N on the surface, namely, an easily ($T < 650$ K) removable form, most likely at the edges of the nitrogen islands, and a particularly strongly-held second one ($T > 650$ K), perhaps the core of newly deposited islands. Again, this explains the mixed behavior cited above in connection with the isotopically mixed beams.

The TPD data from the three-cycle experiments can be easily quantified. The results are presented in the inset of Fig. 11 for two cases, for $\Delta t_2 = 40$ and 100 s (solid circles). As expected, more ^{15}N is detected on the surface after longer exposures to the second $^{15}NO + CO$ beam. Also, those

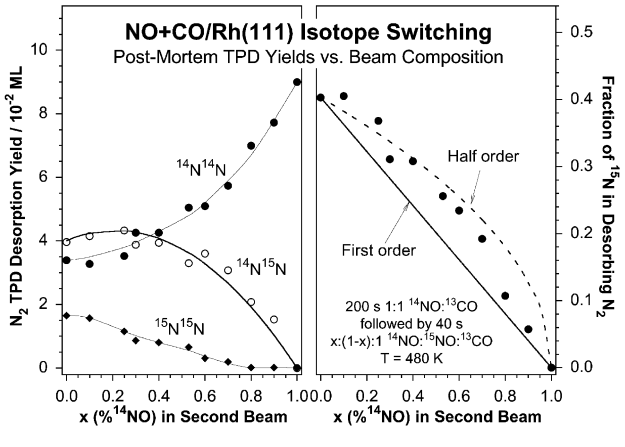

Fig. 9 Left: Molecular nitrogen desorption yields in post-mortem TPD experiments as a function of ^{14}NO fraction (x) in the second molecular beam of the experiments with $^{14}NO + {}^{15}NO + {}^{13}CO$ mixtures reported in Figs. 6, 7, and 8. The solid thick line through the $^{14}N^{15}N$ data corresponds to a calculation assuming a combination of reactions at the periphery of old ^{14}N surface islands and new mixed $^{14}N + {}^{15}N$ islands (see text); the others (thin lines) are only provided to help guide the eye. Right: Fraction of ^{15}N in the desorbing N_2 as a function of x. The behavior can be described by a kinetic law somewhere between first (solid line) and half (broken line) order.

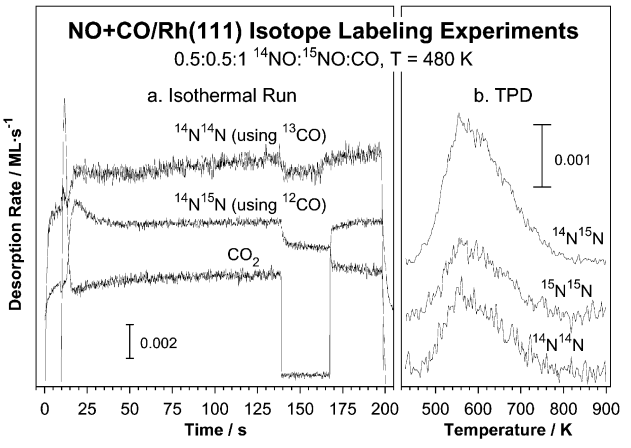

Fig. 10 Raw data from isotope switching isothermal kinetic molecular beam experiments with Rh(111) at 480 K with 0.5 : 0.5 : 1 $^{14}NO:{}^{15}NO:CO$ mixtures. Results from two runs, with ^{12}CO and ^{13}CO, are shown here. The CO_2 trace corresponds to the average from both ($^{12}CO_2$ and $^{13}CO_2$, respectively), and was used to assure the reproducibility of these kinetic measurements. The steady-state rates, determined by the drops in signal upon beam blocking at $t = 140$ s, amount to 0.0008 and 0.0016 ML s^{-1} for $^{14}N^{14}N$ and $^{14}N^{15}N$, as expected based on statistical grounds. Moreover, the shapes and T_{max} of all the post-mortem nitrogen TPD peaks are quite similar, indicating complete intermixing of ^{14}N and ^{15}N on the surface. The yields follow the $1:2:1\ ^{14}N^{14}N:{}^{14}N^{15}N:{}^{15}N^{15}N$ ratios of a fully isotopically random layer as well.

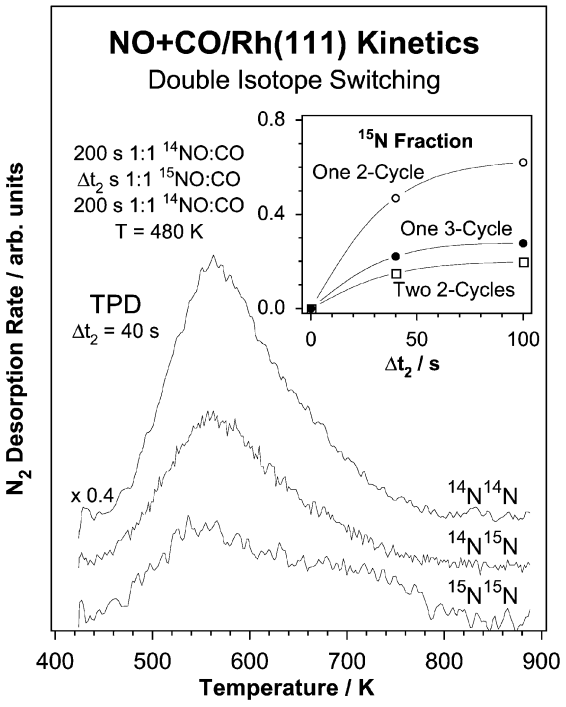

Fig. 11 Main frame: typical post-mortem N_2 TPD traces after a three-cycle isothermal kinetic molecular beam experiments, with identical $^{14}NO + CO$ (200 s), $^{15}NO + CO$ ($\Delta t_2 = 40$ s), and back to $^{14}NO + CO$ (200 s), mixtures. Inset: calculated fractions of ^{15}N left on the surface as a function of Δt_2 (filled circles), compared with those measured after simple two-cycle experiments with the same delay times (open circles) and with estimates from two two-cycle experiments, with Δt_2 and 200 s (open squares). It can be seen there that the three-cycle data cannot be explained simply by two two-cycle runs.

fractions are significantly lower than those obtained after the corresponding two-cycle experiments (open circles), because the third beam is clearly capable of replacing some of the newly deposited ^{15}N with ^{14}N. However, the coverages measured in these three-cycle experiments are not easily explained by the data from two-cycle studies (open squares), by combining the results from exposures of ^{14}N-covered surfaces to $^{15}NO + CO$ beams for a Δt period with those after 200 s exposures in the same type of ^{14}NO to ^{15}NO switching experiments (to account for the third cycle, where some of the ^{15}N is displaced back by new ^{14}N). In fact, there is an *ca.* 30% discrepancy between the two sets of data, the numbers from the three-cycle experiments being consistently larger than those from the two-cycle calculations. Most of this excess ^{15}N can be accounted for by the high-temperature $^{15}N^{15}N$ TPD peak, which suggests that new islands do indeed develop in the second part of the experiment with the $^{15}NO + CO$ beam.

4. Discussion

Based on our previous kinetic experiments with $NO + CO$ molecular beams on Rh(111),[22,32–41] a model was put forward for the mechanism of nitrogen monoxide reduction based on the growth of atomic nitrogen surface islands.[33,38,39] It was suggested that there is a preferential reaction between the N atoms on the edges of those islands and new incoming NO molecules to form N–NO intermediates, which subsequently dissociate to produce molecular nitrogen.[35,39] Two key experimental observations were pivotal in the development of this model. First, the TPD obtained after isotope switching experiments display non-statistical yield distributions and different peak shapes and temperature maxima for the three molecular nitrogen isotopologues ($^{14}N^{14}N$, $^{14}N^{15}N$, and $^{15}N^{15}N$). This provides a clear indication that nitrogen atoms are distributed on the surface in a non-random fashion, and that they have limited mobility up to the temperature needed for their recombination and desorption. In addition, the ^{14}N deposited by initial exposures of the surface to $^{14}NO + CO$ beams are almost exclusively removed as $^{14}N^{15}N$ once the beam is switched to $^{15}NO + CO$ mixtures. Given that virtually no $^{14}N^{14}N$ is produced even right after the isotope switchover, when the surface is covered almost exclusively with ^{14}N, a new incoming NO molecule must be involved in the production of molecular nitrogen.

The studies reported here expand on the evidence that supports our islanding model, but also point to some subtle complications to the initial picture. For one, the kinetics of molecular nitrogen formation in the transient immediately after blocking the exposure of the Rh(111) surface to the $NO + CO$ beam is not simple, displaying at least two distinct regimes: a rapid decay within the first couple of seconds followed by a slower first-order desorption (Fig. 3). Because this reaction takes place in the absence of fresh NO molecules from the gas phase, it is reasonable to propose that at least the long-term desorption seen here corresponds to the recombination of two nitrogen surface atoms. The first-order kinetics can be explained by the low mobility of the nitrogen atoms, which forces the recombination to occur between adjacent adsorbates exclusively. Atomic nitrogen recombination can indeed take place, albeit at a lower rate than the steady-state catalytic production of N_2 with $NO + CO$ mixtures.[41]

On the other hand, the first-order transient process only accounts for about half of the total nitrogen that desorbs isothermally after the beam is blocked. An additional ~0.007 ML atomic nitrogen can only be displaced by reintroduction of the reaction mixture (Fig. 4), not to mention the 0.17 ML of strongly-held adsorbates present as surface islands, which only desorb when heating to higher temperatures.[32] The molecular nitrogen displaced by the new $^{15}NO + CO$ beam is mostly in the form of $^{14}N^{14}N$ (Fig. 1), a result that points to the presence of ^{14}N–^{14}NO intermediates on the surface long after the $^{14}NO + CO$ beam is replaced. It could be argued that $^{14}N + {}^{14}N$ recombination may be facilitated by the CO in the new beam, except that previous experiments have indicated that the CO coverage on the surface under the conditions of the reaction is negligible.[21,32,34,49] What is clear is that the dissociation of the surface N–NO intermediates is affected by neighboring coadsorbates. As the initial beam is switched off, the species adsorbed on those neighboring sites desorb, but when the new beam is introduced, they repopulate, and exert an indirect influence in the rate of N–NO dissociation *via* a change in the adsorption energy of that intermediate. This type of coverage-dependent kinetic effect has already been fully characterized for several surface reactions,[42,43] and is also operative during the recombination of atomic nitrogen in this system.[41]

The complexity of the kinetics of molecular nitrogen formation from the catalytic reduction of NO on Rh(111) is further evidenced by the results obtained here with mixed isotope beams. An approximately second-order behavior was seen after 40 s of switching the initial $^{14}NO + CO$ beam with similar mixtures of $x : (1 - x) : 1\ ^{14}NO : {}^{15}NO : CO$ (Fig. 6), as expected during steady state, but a more complex behavior was seen after a delay of only 15 s. A linear dependence of the $^{14}N^{14}N$ production rate on ^{14}NO content in the replacing beam was seen in that case, consistent with the reaction of one new NO molecule with the nitrogen atoms predeposited on the surface. The lower absolute rate values observed after that time delay, as compared to those observed after longer delays, and the minimum amount of ^{14}NO required in the mixture for the production of any $^{14}N^{14}N$ are, however, not yet understood. What is clear is that the shapes and position of the post-mortem TPD spectra indicate a higher degree of intermixing

between the ^{14}N and ^{15}N atoms on the surface than in the case where the $^{14}NO + CO$ beam is directly replaced with $^{15}NO + CO$ (Figs. 7 and 8). This means that the behavior observed with the mixtures is the result of a combination of reactions between incoming ^{15}NO molecules and preexisting ^{14}N surface atoms on the one hand, and the build up of new islands *via* the decomposition of NO molecules from the new beam on the other. The fit of the $^{14}N^{15}N$ yields as a function of ^{14}NO fraction in the second beam reported in Fig. 9 provides an estimate ratio of 1 : 2 for the relative importance of those two processes. The data from the three-cycle experiments also support this explanation, although it places a relatively lower importance to the formation of new islands.

5. Conclusions

A series of isotope labeling isothermal kinetic experiments were carried out with molecular beams in order to expand on our previous picture of the reaction mechanism of NO reduction on rhodium surfaces. The new results are consistent with the model advanced previously where a critical coverage of atomic nitrogen builds up on the surface before the production of molecular nitrogen. These N atoms cluster in surface islands, allowing for reactivity only at the periphery of those two-dimensional structures. N_2 formation takes place *via* the initial formation of N–NO intermediates between those edge nitrogen atoms and new NO reactants. Previous analysis of the kinetic data puts the average size of those islands at a diameter of about nine atoms, and a probability for access to the second layer of about 15%.

Fast switching experiments as well as newly designed kinetic runs with isotope mixtures provided additional subtleties to this model. First of all, detailed analysis of the kinetics of molecular nitrogen production during the transient immediately following the interruption of the exposure of the Rh(111) surface to the reaction mixture revealed at least two distinct kinetic regimes. A slow first-order process, likely to be associated with direct recombination of nitrogen atoms,[41] can only account for less than half of the steady-state N_2 production rate. The rest of the N_2 is produced by decomposition of an N–NO intermediate, which remains on the surface after the switching off of the first beam, and only reacts when in the presence of new adsorbed molecules. In fact, the displacement of ^{14}N left behind by initial exposure of the surface to $^{14}NO + CO$ by subsequent dosing with similar $^{15}NO + CO$ mixtures includes the fast desorption of a small amount of $^{14}N^{14}N$. The extent of the purely ^{14}N-labeled molecular nitrogen displaced after isotope switching in the reaction mixture decreases slowly with time, and is proportional to its total yield.

The use of ^{14}NO and ^{15}NO mixtures in the second beam of our isothermal kinetic isotope switching measurements added to our interpretation of the kinetics of this system. After reasonably long times after the beam switchover, the rate of $^{14}N^{14}N$ production was found to follow a second-order dependence on the fraction of ^{14}NO in the beam, as expected during steady-state conditions. After shorter delays, however, the observed behavior is more complex, resembling a linear rate law with the requirement of a minimum ^{14}NO fraction in the beam for any $^{14}N^{14}N$ to be produced. The resulting $^{14}N + ^{15}N$ surface layers appeared to be more intimately mixed than when switching from $^{14}NO + CO$ to pure $^{15}NO + CO$ beams, as indicated by the more similar peak shapes and temperature maxima among the three molecular nitrogen isotopologues in the post-mortem TPD acquired in the former case. The data obtained in these experiments were interpreted as being the result of a combination of reactions of new nitrogen monoxide molecules at the periphery of previously deposited ^{14}N islands with the growth of new isotopically mixed atomic nitrogen surface clusters.

Acknowledgements

Funding for this research was provided by a grant from the National Science Foundation. Additional funding came from a Los Alamos-University of California joint program.

References

1 R. J. Farrauto, R. M. Heck and B. K. Speronello, *Chem. Eng. News*, 1992, **Sept. 7**, 34.
2 A. M. Thayer, *Chem. Eng. News*, 1992, **March 9**, 27.
3 M. Shelef and G. W. Graham, *Catal. Rev. Sci. Eng.*, 1994, **36**, 433.
4 T. W. Root, L. D. Schmidt and G. B. Fisher, *Surf. Sci.*, 1983, **134**, 30.
5 T. W. Root, L. D. Schmidt and G. B. Fisher, *Surf. Sci.*, 1985, **150**, 173.
6 V. P. Zhdanov and B. Kasemo, *Surf. Sci. Rep.*, 1997, **29**, 31.
7 T. W. Root, G. B. Fisher and L. D. Schmidt, *J. Chem. Phys.*, 1986, **85**, 4687.
8 S. B. Schwartz, G. B. Fisher and L. D. Schmidt, *J. Phys. Chem.*, 1988, **92**, 389.
9 C. H. F. Peden, D. W. Goodman, D. S. Blair, P. J. Berlowitz, G. B. Fisher and S. H. Oh, *J. Phys. Chem.*, 1988, **92**, 1563.
10 C. H. F. Peden, D. N. Belton and S. J. Schmieg, *J. Catal.*, 1995, **155**, 204.
11 D. N. Belton and S. J. Schmieg, *J. Catal.*, 1993, **144**, 9.
12 L. H. Dubois, P. K. Hansma and G. A. Somorjai, *J. Catal.*, 1980, **65**, 318.
13 W. C. Becker and A. T. Bell, *J. Catal.*, 1983, **84**, 200.
14 R. E. Hendershot and R. S. Hansen, *J. Catal.*, 1986, **98**, 150.
15 B. K. Cho, B. H. Shanks and J. E. Bailey, *J. Catal.*, 1989, **115**, 486.
16 B. K. Cho, *J. Catal.*, 1994, **148**, 697.
17 K. Y. S. Ng, D. N. Belton, S. J. Schmieg and G. B. Fisher, *J. Catal.*, 1994, **146**, 394.
18 S. H. Oh, G. B. Fisher, J. E. Carpenter and D. W. Goodman, *J. Catal.*, 1986, **100**, 360.
19 S. H. Oh and J. E. Carpenter, *J. Catal.*, 1986, **101**, 114.
20 S. H. Oh, *J. Catal.*, 1990, **124**, 477.
21 H. Permana, K. Y. S. Ng, C. H. F. Peden, S. J. Schmieg, D. K. Lambert and D. N. Belton, *J. Catal.*, 1996, **164**, 194.
22 M. Aryafar and F. Zaera, *J. Catal.*, 1998, **175**, 316.
23 L. A. DeLouise and N. Winograd, *Surf. Sci.*, 1985, **159**, 199.
24 H. J. Borg, J. F. C.-J. M. Reijerse, R. A. van Santen and J. W. Niemantsverdriet, *J. Chem. Phys.*, 1994, **101**, 10 052.
25 T. W. Root, G. B. Fisher and L. D. Schmidt, *J. Chem. Phys.*, 1986, **85**, 4679.
26 C.-T. Kao, G. S. Blackman, M. A. Van Hove, G. A. Somorjai and C.-M. Chan, *Surf. Sci.*, 1989, **224**, 77.
27 D. N. Belton, C. L. DiMaggio, S. J. Schmieg and K. Y. S. Ng, *J. Catal.*, 1995, **157**, 559.
28 D. N. Belton, C. L. DiMaggio and K. Y. S. Ng, *J. Catal.*, 1993, **144**, 273.
29 Y. Li and M. Bowker, *Surf. Sci.*, 1996, **348**, 67.
30 M. Bowker, Q. Guo, Y. Li and R. W. Joyner, *J. Chem. Soc., Faraday Trans.*, 1995, **91**, 3663.
31 G. Prevot, O. Meerson, L. Piccolo and C. R. Henry, *J. Phys.: Condens. Matter*, 2002, **14**, 4251.
32 C. S. Gopinath and F. Zaera, *J. Catal.*, 1999, **186**, 387.
33 F. Zaera and C. S. Gopinath, *J. Chem. Phys.*, 1999, **111**, 8088.
34 C. S. Gopinath and F. Zaera, *J. Phys. Chem. B*, 2000, **104**, 3194.
35 F. Zaera and C. S. Gopinath, *Chem. Phys. Lett.*, 2000, **332**, 209.
36 F. Zaera and C. S. Gopinath, in *Proceedings of the 12th Inernational Congress of Catalysis, Granada, Spain, July 9–14, 2000 (Studies in Surface Science and Catalysis Series, Vol 130)*, ed. A. Corma, F. V. Melo, S. Mendioroz and J. L. G. Fierro, Elsevier, Amsterdam, 2000, pp. 1295.
37 V. Bustos, C. S. Gopinath, R. Uñac, F. Zaera and G. Zgrablich, *J. Chem. Phys.*, 2001, **114**, 10 927.
38 F. Zaera, S. Wehner, C. S. Gopinath, J. L. Sales, V. Gargiulo and G. Zgrablich, *J. Phys. Chem. B*, 2001, **105**, 7771.
39 F. Zaera and C. S. Gopinath, *J. Mol. Catal. A*, 2001, **167**, 23.
40 C. S. Gopinath and F. Zaera, *J. Catal.*, 2001, **200**, 270.
41 F. Zaera and C. S. Gopinath, *J. Chem. Phys.*, 2002, **116**, 1128.

42 F. Zaera, *Prog. Surf. Sci.*, 2001, **69**, 1.
43 F. Zaera, *Acc. Chem. Res.*, 2002, **35**, 129.
44 F. Zaera, *J. Phys. Chem. B*, 2002, **106**, 4043.
45 J. Liu, M. Xu, T. Nordmeyer and F. Zaera, *J. Phys. Chem.*, 1995, **99**, 6167.
46 H. Öfner and F. Zaera, *J. Phys. Chem.*, 1997, **101**, 396.
47 F. Zaera, J. Liu and M. Xu, *J. Chem. Phys.*, 1997, **106**, 4204.
48 F. Zaera, *Int. Rev. Phys. Chem.*, 2002, **21**, 433.
49 M. J. P. Hopstaken, W. J. H. van Gennip and J. W. Niemantsverdriet, *Surf. Sci.*, 1999, **435**, 69.